PROPELLANTLESS DEORBITING OF SPACE DEBRIS BY BARE ELECTRODYNAMIC TETHERS

Juan R. Sanmartin, juanr.sanmartin@upm.es
Shaker B. Khan, bayajid.khan@upm.es, **Claudio Bombardelli**, claudio.bombardelli@upm.es
Universidad Politecnica de Madrid, Spain,
Enrico C. Lorenzini, enrico.lorenzini@unipd.it
Giacomo Colombatti, giacomo.colombatti@unipd.it, **Denis Zanutto**, denis.zanutto@studenti.unipd.it
Universitá degli Studi di Padova, Italy
Jean-Francois Roussel, roussel@onera.fr, **Pierre Sarrailh**, pierre.sarrailh@onera.fr
ONERA, Toulouse,France
John D. Williams, john.d.williams@colostate.edu
Garrett E. Metz, gmetz@rams.colostate.edu, **James K. Thomas,** jkthomas@engr.colostate.edu
Colorado State University, Fort Collins/CO, United States
Jose A. Carrasco, joseacarrasco@emxys.com, **Francisco Garcia de Quiros,** fgarciaq@emxys.com
Embedded Instruments and Systems S.L., Elche, Spain
Olaf.Kroemer, Olaf.Kroemer@dlr.de
Roland.Rosta, Roland.Rosta@dlr.de, **Tim van Zoest**, Tim.Zoest@dlr.de
DLR German Aerospace Center, Bremen, Germany
Joseba Lasa, joseba.lasa@tecnalia.com, **Jesus Marcos**, jesus.marcos@tecnalia.com
Fundacion Tecnalia, San Sebastian, Spain

A 3-year Project started on November 1 2010, financed by the European Commision within the FP-7 Space Program, and aimed at developing an efficient de-orbit system that could be carried on board by future spacecraft launched into LEO, will be presented. The operational system will deploy a thin uninsulated tape-tether to collect electrons as a giant Langmuir probe, using no propellant/no power supply, and generating power on board. This project will involve free-fall tests, and laboratory hypervelocity-impact and tether-current tests, and design/Manufacturing of subsystems: interface elements, electric control and driving module, electron-ejecting plasma contactor, tether-deployment mechanism/end-mass, and tape samples. Preliminary results to be presented involve: *i*) devising criteria for sizing the three disparate tape dimensions, affecting mass, resistance, current-collection, magnetic self-field, and survivability against debris itself; *ii*) assessing the dynamical relevance of tether parameters in implementing control laws to limit oscillations in /off the orbital plane, where passive stability may be marginal; *iii*) deriving a law for bare-tape current from numerical simulations and chamber tests, taking into account ambient magnetic field, ion ram motion, and adiabatic electron trapping; *iv*) determining requirements on a year-dormant hollow cathode under long times/broad emission-range operation, and trading-off against use of electron thermal emission; *v*) determining requirements on magnetic components and power semiconductors for a control module that faces high voltage/power operation under mass/volume limitations; *vi*) assessing strategies to passively deploy a wide conductive tape that needs no retrieval, while avoiding jamming and ending at minimum libration; *vii*) evaluating the tape structure as regards conductive and dielectric materials, both lengthwise and in its cross-section, in particular to prevent arcing in triple-point junctions.

I. INTRODUCTION

In 1972 Hans Alfven observed that the electric field at the highly conductive magnetized plasma around a wire travelling in the solar wind is negligible in the plasma frame. The nonrelativistic electric-field transformation between two reference frames moving with plasma and wire respectively, shows a so called *motional* field $\overline{E}_m$ (wire-to-plasma relative velocity × ambient magnetic field $\overline{B}$) to be present, in the frame of the wire, in the ambient plasma around.

The electromotive force $E_m L$ could drive current in a wire of length L, and make powering electrical thrusters, for propulsion in interplanetary travel, possible. Actually, a generalized Alfven scheme could do away with the thrusters. The magnetic (Lorentz) force on the induced current would itself drag the conductor, which would tend to approach the local velocity of the solar wind. This is just a dissipative kinetic process; drag from streaming air, if present, would have the same effect.

In a somewhat similar way, an orbiting tether/spacecraft uses Lorentz drag on the tether current,

arising from the motion relative to the corotating magnetized plasma, which induces the current. An electrodynamic tether or ED-tether system here considered for 'rapid' deorbiting of satellites at end of mission, requiring no propellant and no power supply while being capable of generating power for on board use while deorbiting, is a perfect application for the slow, ambient dependent, average action of the Lorentz force.

The potential along the tether, in its frame, will follow the simple ohmic law, and will actually be nearly uniform in the simplest case of low enough current. Outside the tether, the plasma will be equipotential in its corotating own frame, but will be given in the tether frame by the Lorentz transformation determining the motional field,

$$\overline{E}(\textit{tether frame}) \approx \overline{E}(\textit{tether frame})$$
$$-\overline{E}(\textit{plasma frame}) = (\overline{v}_{orb} - \overline{v}_{cor}) \times \overline{B} \qquad [1]$$

with $v_{cor} \sim v_{orb}/16 << v_{orb}$. In the simplest case, with both $\overline{B}$ and $\overline{v}_{orb}$ horizontal, the motional field is vertical (upwards for prograde orbits). The tether itself may lie vertical, along the gravity gradient.

2. MISSION AND PLASMA PARAMETERS

The deorbit-mission impulse can be approximately written as

$$M_{sat}\Delta v_{orb} = I_{av}L \times (E_m / v_{orb})\Delta t \qquad [2]$$

where I_{av} is tether current averaged over its length L, all values are averages over the entire deorbit operation, and Δt is its overall duration. The above impulse presents a broad range of values of about 1½ orders of magnitude. We will consider M_{sat} values ranging from 400 kg to 6000 kg, thus varying by a factor of 15, whereas Δv_{orb}, as given by

$$\Delta v_{orb} \approx \sqrt{\frac{GM_E}{R_E}} \times \frac{|\Delta H|}{2R_E} \qquad [3]$$

where H is orbit altitude, has a limited representative range, covering values within a factor of 2, for deorbiting from 900 and 1500 km, say. Note that only at low orbit inclinations do we have $E_m / v_{orb} \approx B$, with E_m about 150 V/km. At high inclinations, magnetic field $\overline{B}$ and orbital velocity $\overline{v}_{orb}$ can be nearly parallel, a characteristic value for $E_m / v_{orb}B$ being the tilt angle of the Earth magnetic field, which is about 0.2, resulting in a value E_m less than 30 V/km, leading to a greater Δt.

Although they depend on night/day, solar Max/Min conditions, we may say, synoptically, that plasma density N roughly ranges from as low as 10^4 to above 10^6 cm^{-3}, while composition is first dominated by oxygen and finally by hydrogen. Electron temperature T_e is about 0.1-0.2 eV, and the temperature ratio T_i / T_e is typically about 1.

Ram energy for oxygen, at the lower altitudes, is about $½\, m_i v_{rel}^2 \sim 4.5$ eV, and as low as 0.25 eV for hydrogen, at the higher altitudes, for which it is close to the ion thermal energy, suggesting a negligible ram effect, if any. As regards plasma neutrality, electrical screening of charges, and potentials due to charges, is determined by the Debye length

$$\lambda_D \propto \sqrt{T_e / N_e} \sim 3 - 9 \text{ mm}$$

The electron thermal gyroradius $l_e \propto \sqrt{T_e} / B \sim 25 - 30$ mm, is reasonably large when compared to the Debye length.

3. TETHER SELECTION

3.1 General considerations

Clearly, the tether as a system for deorbiting will be ultimately destroyed at reentry; it will therefore be an expendable tether. This also means that tether retrieval, an operation that is dynamically complex, would not be required. To ease no-spin deployment, ending in libration, a non-conductive segment having high strength and low deployment tension, might precede the bare tether at the anodic end, acting as stabilizing tether 'pilot', until a substantial gravity-gradient force has been attained.

As it was the case for the NASA *ProSEDS* tether, a mission cancelled following the *Columbia* tragedy, and as regards the tether materials structure, a bare tether made of aluminium, as later considered because of its high conductivity-to-density ratio, might require some coating with low surface resistive, and high emissivity, to keep the tether from excessive heating; aluminium alloys, such as the 1350-0, have low emissivity, around 0.2. Such coating could also tolerate atomic oxygen, which, anyway, might raise issues at a late, faster stage in deorbiting.

In case the plasma contactor (hollow cathode) ejecting electrons at the cathodic end is off at some point, the tether might be electrically floating (i. e., have zero current at both ends), and could be polarized highly negative over most of its length to balance ion collection against electron collection. If the bare tether is insulated over some segment at the cathodic end, to avoid short-circuits at the deployer, a triple point at the junction would exist once deployed, with the bare tether highly negative with respect to the plasma. Laboratory tests exhibited arcs when bias reached a fraction of kV. A short semiconductor sleeve at the junction, to smooth the local electric field, was found to suppress arcs.

3.2 Bare tether versus insulated tether

Both NASA tethers TSS1 and TSS1R carried insulation throughout, and a conductive big sphere of radius $R = 0.8$ m at the anodic end to capture electrons. The maximum current collected by a spherical probe under isotropic conditions is the so called OML current, reading

$$I_{OML}(3D) = I_{th}\left(1 + \frac{e\Delta V}{kT}\right) \approx I_{th} \times \frac{e\Delta V}{kT} \qquad [4]$$

for the high probe bias ΔV of interest. A typical bias ratio at the anodic tether end might be as high as 10^4. Unfortunately, the 3D-OML current is only reached at vanishing R/λ_D ratio; then, the random current, $I_{th} \propto R^2$, would itself be fully negligible. The R/λ_D ratio for the TSS1 / TSS1R sphere was of order of 10^2. The Debye sheath is then extremely thin, current keeping close to the random value, [1] - [3].

The high-bias 2D-OML current appropriate for a cylindrical collector such as a bare tether is small compared with the value in (4) at equal collecting area,

$$I_{OML}(2D) \approx I_{th} \times \sqrt{\frac{\pi\, e\Delta V}{4kT}}$$

$$= LeN\frac{p_t}{\pi}\sqrt{\frac{2e\Delta V}{m_e}} \qquad [5]$$

This OML-current law, yielding currents as high as 10^2 times the random value, applies, however, to a cylinder radius R less than some *maximum* radius R_{max} that is comparable to λ_D, which will actually be larger than the radius of any practical tether. Further, a tether with radius λ_D and $L \sim 10$ km, would have a collecting area about 30 times the area of a sphere of radius 0.8 m; this more than balances the fact that the length-averaged tether bias will be a (high) fraction of maximum bias, at the anodic end.

IV. TETHER SYSTEM DESIGN

(*i*) Tether Sizing

The 2D-OML collection law is known to apply to any cylinder of cross-section contour convex everywhere, for which one just uses its actual perimeter for p_t in Eq.(5), [4]. A particular case of interest is a thin tape, which has the largest perimeter and thus current collection capability for given cross-section area. If w and h are tape width and thickness respectively, with the ratio $\varepsilon \equiv h/w << 1$, a tether of circular cross section of equal mass and length, will have a radius $R = w\sqrt{(\varepsilon/\pi)}$ and its cross-section perimeter smaller than that of the tape, which is about $2w$, in the small ratio $\sqrt{(\pi\varepsilon)}$.

The high bias of interest makes the charge density have no effect over a large region around the tape, where the Laplace equation applies. Farther away within the large sheath, potential and plasma density reach circular symmetry. One then readily finds

$$w_{max} = 4R_{max}.$$

For a representative $w = 20$ mm, $h = 0.05$ mm, $\varepsilon = 1/400$ tape, the corresponding radius would be $R = 1/\sqrt{\pi}$ mm. The round wire-to-tape current ratio is then $\sqrt{\pi}/20$, or about 0.1. For given mission impulse, using a tape for deorbiting would reduce the required time to 10 % of the time required by a round tether of equal mass and length.

The above result may stand in the presence of ohmic effects up to here ignored. The length-averaged current determining the Lorentz force, normalized with the short-circuit current $\sigma_c E_m A_t$, reads

$$I_{av} / \sigma_c E_m A_t = i_{av}(L / L_*)$$

where we defined a length L_* by writing

$$\Rightarrow \qquad L_* \equiv l^{1/3}(2A_t / p_t)^{2/3}$$

where A_t is tether cross-section area, and

$$l \propto E_m / N_e^2$$

is certain auxiliary length. In principle, at large L / L_* the average current I_{av} reaches the limiting ohmic-dominated, short-circuit value, which would be equal

for round wire and tape of equal cross section area. Since

$$\left(2A_t / p_t\right)^{2/3} \Rightarrow R^{2/3} \text{ for round wires}$$
$$\Rightarrow h^{2/3} \ (<< R^{2/3}) \text{ for tapes,}$$

however, the ratio L_* /L for a tape will be much larger than the value of L_* /L for its corresponding round wire.

Tether current may thus be ohmic-dominated for tapes while not for wires. Comparing deorbiting times at given mission impulse for round and tape tethers of equal volume (mass) then leads to the previous result of much faster deorbiting by the tape for a broad range of conditions.

In deorbiting, a tether may collide with big objects in space, be live satellites or second rocket stages, say of size above 1 or 10 m, which are tracked in space. The tether will itself be a debris for a live satellite, which must manoeuvre to avoid being hit by the tether. Further, any big body will be also a debris for the tether. The collision risk is roughly characterized by the product of tether front-area and deorbiting time, and may be shown typically comparable for round wires and tapes.

Independently, numerous small debris (its diameter δ << 1m, say) may cut the tether with no possible allowed manoeuvre. In comparing round versus tape tethers as regards the number of fatal impacts N_c, to be later used in a Poisson probability distribution, we may use a simple formula frequently used to estimate N_c for a round tether,

$$\frac{N_c}{L\Delta t} \equiv \dot{n}_c = \int_{\delta_m}^{\delta_\infty} \frac{-dF}{d\delta} d\delta \, D_{eff}(\delta).$$

Here δ_∞ is 1m, say, $D = 2R$ is tether diameter and δ_m is the minimum debris diameter that may be fatal on impact to the tether. Typically one writes δ_m as some fraction of tether diameter, $f_m D$, the value of f_m taken from energy considerations and from observations of grounded satellites surface, showing the effects of debris impacts in space.

D_{eff}, written as $D + \delta - \delta_c$, is an *effective* diameter for the tether as target, which takes into account that debris, at difference with atoms or molecules, cannot be considered as having no macroscopic size. The effective diameter is less than $D + \delta$, however, because just a bruising impact will not be effective in cutting the tether. This is represented by the term δ_c again written as $f_c D$, often setting $f_c = f_m$. As regards $F(\delta)$, this is the cumulative debris flux, or number of debris with size ranging from δ to some large size, usually 1 m, crossing the unit area in unit time. The cumulative debris flux depends, in particular, on orbit altitude and inclination.

Both NASA and ESA have complex models of debris flux, called ORDEM and MASTER respectively. In general the ORDEM model presents higher flux for the small debris range, say below 1 cm. To be conservative in a simplified calculation of the number of fatal impacts, we used the ORDEM model to compare values for round and tape tethers of equal mass. The tape may be said to present an effective "diameter" $w'(\theta) \equiv w(\cos\theta + \varepsilon \sin\theta)$, where w is the tape width, ε is the ratio between tape thickness and width, and θ is the angle between debris relative velocity and the perpendicular to a tape side. One must integrate over the full range of angles to get the number of fatal impacts for a tape.

Use of tapes, as against use of round tethers of equal mass, is finally found to reduce considerably the total fatal-impact count, because both i) the deorbiting time and ii) the fatal impact rate are reduced. A comparison was carried out for multiple values of altitude and inclination, with similar results throughout, showing a reduction on number of fatal impacts by about two orders of magnitude.

Reduction i), is previously discussed, arises from the greater collection capability of the tape, which has a larger perimeter, if the round tether does not reach the ohmic-limited regime, where current would be just determined by mass. Reduction ii) arises from the much lower flux at the "effective" width presented by the tape, except for near edgewise impacts, for which, one can show that very small debris to consider bring too little energy to cut the tether throughout its width.

(*ii*) Tether Dynamics

Important topics in technically developing a system to deorbit space debris through passive electric propulsion involve studying its dynamics and control, and analysing its deorbit performance vs. driving parameters. This requires developing specialized computer codes of two kinds: (1) a simplified dynamics model that can run very efficiently in using it for parametric analyses and (b) a more complete model that simulates the elastic dynamics of the tether system. In the simplified code, tether motion is limited to libration dynamics and, consequently, the tether is modeled as a rigid bar. The more accurate code models the tether with a series of massive lumps connected by springs and dashpots and thus it models tether elasticity and its string dynamics.

Both models use up-to-date versions of environmental routines for ionospheric density (IRI-2007), atmospheric density (NRLMSISE-00) and magnetic field (IGRF-2005). The gravity field is a 4x4 model, which is more than sufficient for the purpose of this study. The atmospheric and ionospheric routines are particularly heavy to run on a computer and for this reason the simplified code makes use of interpolated data from those models to run more efficiently while preserving required accuracy.

The simplified code was used to carry out a parametric analysis of system deorbit performance; specifically, to study its dependence on system parameters (tether length and width), value of tip mass, orbital parameters like altitude, inclination and eccentricity, and environmental parameters like the solar activity that drives ionospheric density. An example of output from the parametric analysis is shown in Fig. 1, which depicts orbital decay vs. time for different values of tether length.

The parametric study has identified the dependence of decay performance on the key system, orbital, and environmental parameters. The analysis will lead to the selection of system parameters that can provide an effective deorbit performance for a broad spectrum of orbital and environmental conditions. The analysis has also highlighted a well-known issue regarding the librational stability of a tether system and its dependence on the input parameters. Stabilization of tether dynamics will be addressed in the next task.

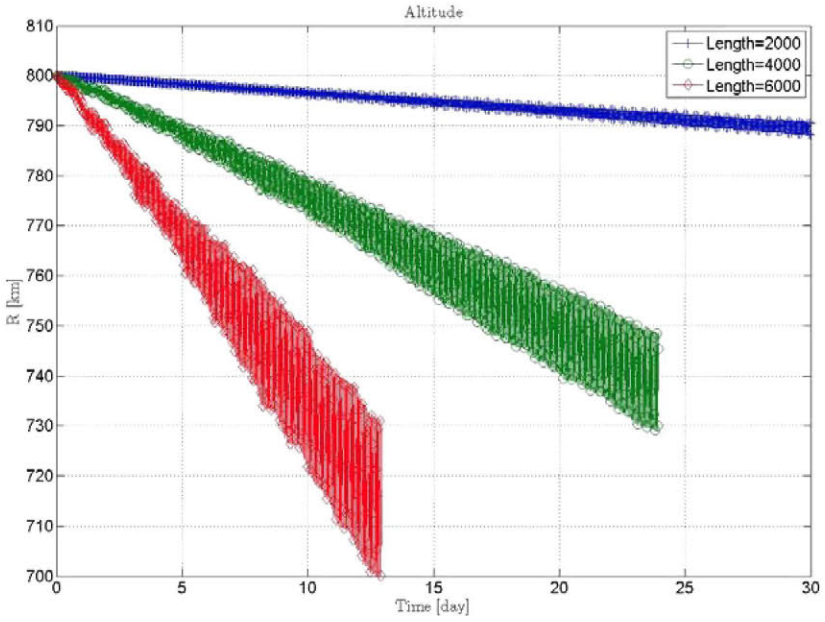

Figure 1 Orbital decay vs. time for different tether lengths (SC mass is 1000 kg)

The more accurate code was validated by comparing simulation results with those available in the literature and through a frequency analysis to highlight the modal components of the elastic vibration modes. The code was used to double check some results of the simpler code, to conclude that it representes well deorbit performance but overestimates the onset of dynamic instabilities.

(*iii*) Tether Current Law

The force generated by a tether is directly proportional to the current flowing through it, whatever the application: deorbiting, orbit rising, power generation, etc. Since the current loop is closed through the plasma, the "quality" of the contact between tether and plasma on both its anode and cathode sections is crucial. It can be expressed as a plasma impedance, or a nonlinear current/voltage-bias characteristics. In the BETs project, cathodic contact is ensured by a hollow cathode acting as plasma contactor, whereas the anode is the tether itself.

Unfortunately, the plasma flow around the tether is in a highly non-trivial regime. The ion flow (in the tether frame) is supersonic, while the tether potential is larger than the ion kinetic energy:

thermal energy < drifting energy < potential energy (to reach the tether).

This regime is known to induce an accumulation of ions ahead of the tether (ions are stopped by the highly positive tether), which may result in turbulence.

With the electrons carrying the tether current, our main interest rests on the electron flow in the anodic sheath. Since there is no actual analytical or semi-analytical model of this highly requiring regime, it is not surprising that comparison of experimental data to approximate models does not show agreement better than typically a factor of two. This directly impacts on the dimensioning of the tether system and needs improvement. The *physic*s at the basis of these discrepancies can be adiabatic trapping of electrons (possibly related to some turbulence) or magnetic effects on electron motion. The existence of slow ions created by charge-exchange with the residual neutrals within plasma tanks in ground tests is another possible source of error in that comparison.

The above issue is studied in the BETs project through both lab tests and numerical simulation approaches. This work is now in progress at ONERA's Space Environment Department in Toulouse. Modeling of the plasma uses the SPIS code [5], [6]. Full PIC (Particle-In-Cell) simulations are being performed and their stability is still under improvement through sophisticated boundary conditions representing more accurately pre-sheath conditions. The next step will be multi-zone modeling, the weakly disturbed plasma region allowing an hybrid model (Boltzmann distribution for electrons with an implicit solver for a nonlinear Poisson equation). Experiments were conducted in ONERA's JONAS plasma tank. Special care was taken of plasma characterization since fast and slow ion populations must be separated to accurately reproduce tank conditions in simulations. Several types of Langmuir probes are used at the same location to allow extracting both ion densities and electron parameters by computer modeling (classical Langmuir probe characteristics is not accurate enough in such a situation). A triple probe was also used for a more extensive characterization of the plasma in space / time dependent analysis. Time oscillations were observed in some regimes (large positive potential of the probe) but still deserve additional analysis.

(*iv*) Hollow Cathode Design

Orificed, thermionic hollow cathodes have been developed and used for a wide variety of applications, including the plasma electron supply for ion and Hall thrusters, and plasma contactors for electromagnetic tethers and spacecraft charging control [7]–[9]. Many theoretical and experimental studies have been performed to understand how orificed hollow cathodes work and how their lifetime and reliability can be modelled.

A typical hollow cathode is shown in Fig.2. The body of the cathode consists of a tantalum tube (6) with a tantalum orifice plate (2). The outer diameter of the orifice plate is 6.35mm, and the orifice diameter is 1.65mm. A porous tungsten insert impregnated with barium-calcium-aluminate (3) is placed inside the tube near the orifice plate. A swaged tantalum heater (4) is coiled around the tube, and a 10-layer radiation shield formed from tantalum foil (5) wrapped around the heater reduces the amount of heat radiated from the cathode thereby minimizing the heater power required for a given tip temperature condition. A second tube

with an orifice plate is placed around the cathode. This electrode is called a keeper (1) and its orifice plate is placed downstream of the cathode and is biased positive of the cathode to initiate a discharge.

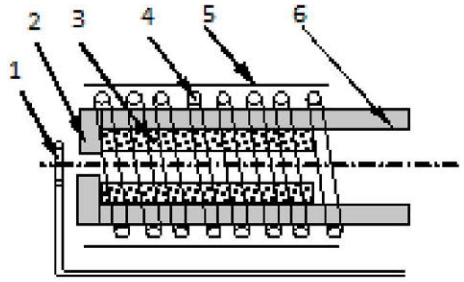

Figure 2 Hollow cathode with insert, heater, radiation shield, and keeper components (only lower half of keeper is shown).

The ion production rate and expellant utilization of a simple hollow cathode assembly can be improved if a discharge chamber is used in combination with a hollow cathode [10]-[11]. The most commonly used magnetic field geometry in discharge chambers used in ion propulsion systems is the ring cusp configuration. A highly effective plasma contactor can be formed by removing the ion acceleration systemfrom the discharge chamber on an ion source [10].

It is possible to transform neutral xenon gas atoms into ions at a rate exceeding 50% of the expellant flow that is introduced into the discharge chamber. The discharge chamber proposed for the BETS Project will be capable of producing ~25 mA of ions under low power and low flow operating conditions. This is approximately 10 to 25 times larger than the ion production rate of a simple hollow cathode discharge operated without a discharge chamber. This ion roduction rate is sufficient to produce a conductive plasma bridge to the ionospheric plasma enabling efficient plasma electron current flow to occur between the lower satellite and the space plasma.

As previously mentioned electrodynamic tethers require low impedance electrical connection to the space plasma. This can occur when the emitted electron current is passed through expanding expellant flow fields, or when open-ended discharge chambers are used to directly produce plasma [12]. The BETS Project discharge chamber equipped plasma contactor will operate with enhanced plasma production and minimum impedance without reliance on the space plasma properties of the orbit or day-night cycle.

Figure 3 contains a simplified block diagram of the HCPC system. The subsystems contained in the HCPC include the expellant control unit (ECU) with the gas tank and heated gas lines that connect the ECU to the plasma contactor, the power control unit (PCU) that contains the power supplies to operate the plasma contactor and the flow control valves in the ECU, the hollow cathode assembly (HCA) with the ring-cusp discharge chamber, and the digital interface unit (DIU)

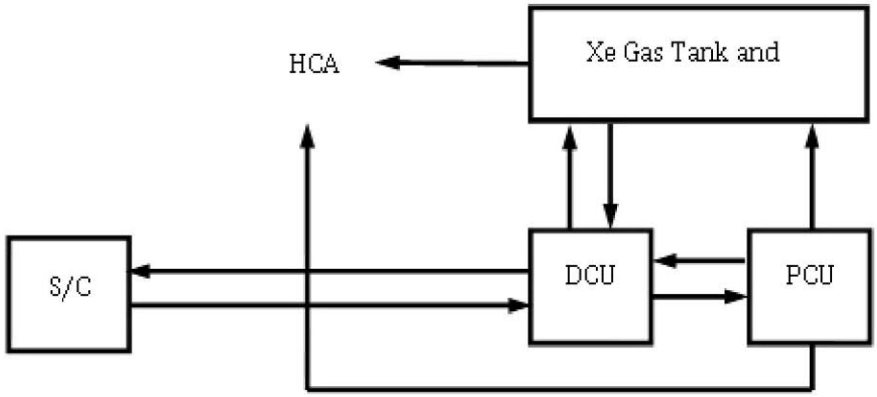

Figure 3 HCPC block diagram

that consists of the communications link and system controller.

Figure 4 displays the electrical schematics of the plasma source-based hollow cathode plasma contactor.

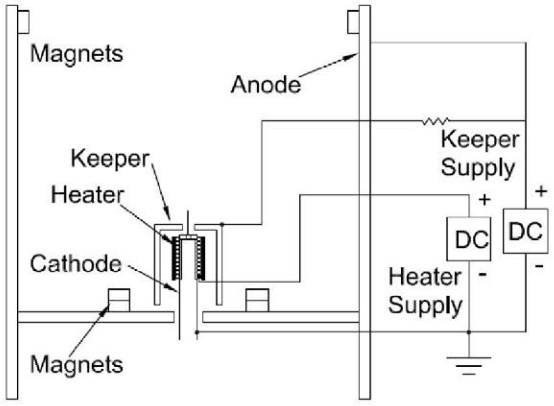

Figure 4 HCPC HCA electrical sketch

(v) Power Module

Main objectives of the power supply under design are providing power to the Hollow Cathode system and dissipating (or possibly regenerating) the electrical energy injected by the electrodynamic tether. The block diagram of the complete power supply is presented in the figure above.

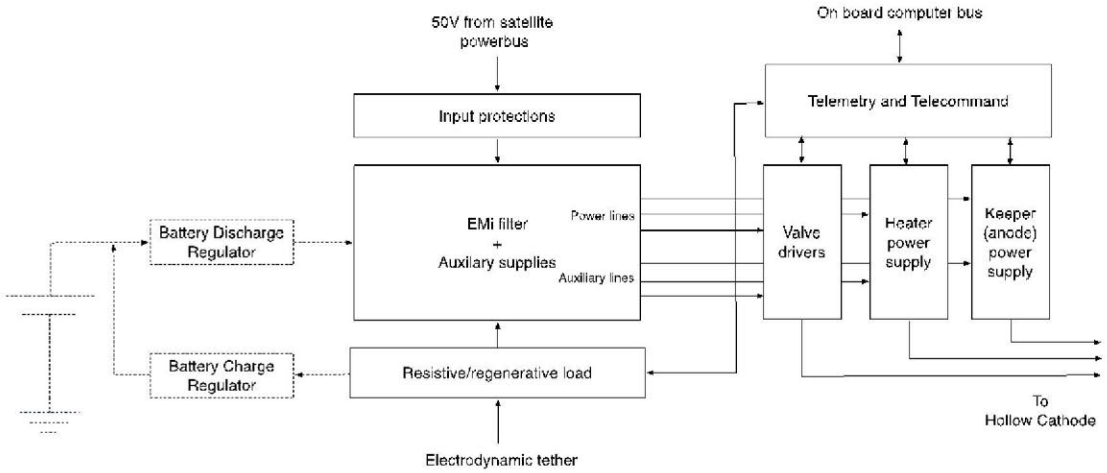

The power supply is directly connected to the satellite power bus, through an EMI filter and mandatory protection elements, and to the on-board computer, which provides power and control to the tether system. The system can be made autonomous by optionally including a battery, and a battery charger, which will be maintained fully loaded by the satellite power bus until the tether is operated at satellite end-of-life. The battery will then supply initial power for the Hollow Cathode start-up, and the system will switch to the electro-dynamic tether regenerative load for subsequent power generation.

The Hollow Cathode requires three power supplies:

- A low voltage and low power supply to operate the electric-valve drivers that supply xenon to its interior.
- A low power supply to provide heat to the Hollow Cathode heater until it reaches nominal operation.
- A high-voltage pulsed-power supply to initiate the cathode operation that turns into a continuous low voltage and low power supply when reaching nominal operation.

A telemetry and control unit completes the set and provides telemetry and operation of the whole system, including autonomous operation if the system is programmed to operate autonomously in controlling tether libration

(*vi*) Tether Deployer

The design goal was to create a universally useable, stand-alone system which does not need much more than a trigger signal and electrical connection of the main spacecraft to keep the system battery charged. Thus, the

whole deorbiting system can be kept operational until the end-of-life of the satellite and even if the whole satellite dies without warning, the deorbiting process could be started autonomously when the power supply of the satellite shuts down and no operation signal is sent to the BETs system.

To find the most suitable deployment concept, research was carried out to determine the state-of-the-art as well as those environmental parameters having greater influence on the overall functionality. Those concepts were conjoined with new deployment ideas, based on the DLR experience in deploying small electrically conductive tethers [13] and flat cables on planetary surfaces [14]. To verify the theoretical studies, seven concepts and concept variations were realized in breadboard units and tested in three different deployment test campaigns considering physical properties like size and mass, required deployment pull-force, event-free unfolding and controllability of the deployment process. The test results were then compared within a rating matrix.

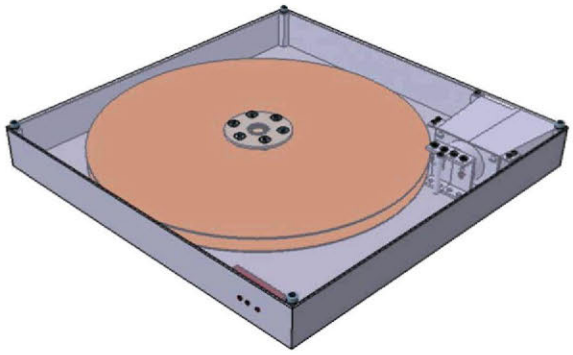

Fig.5 Passive deployment mechanism

The top rated deployment concept has shown the desired result of event-free tether deployment. The tether was unreeled without any twisting or impulsion events proving that entanglement risk is very low and failure during deployment is highly improbable. An important design criterion was striving for simplicity in the entire deployer system, including the release mechanism. In the best-concept case, overall complexity has been kept low by limiting the number of components. Results of measured maximum pull-force have shown that the most promising design concept uses steady and low deployment force.

The only drawback of the concept is that with increasing tether length, in thecase of a highly scaled up mission, the reeled tether becomes a large disc, which might collide with the requirement of BETs system validity for any satellite. This problem may be solved by splitting the full length into more than one reel or by reeling the entire length on a spool with increasing building height.

It has been finally figured out that a purely passive deployment concept may hardly attain the required reliability of the deployment process. To keep reliability high, it has been decided that the two most promising concepts shall be further investigated under the viewpoint of actively-driven deployment via motor or a pulling gas-thruster mechanism.

(*vii*) Tape Design

Different tether alternatives have been analysed, Hoytethers, Amberstrand, ProSEDS, and T-rex, among other systems. At the same time, a deep study of materials used for their manufacture has been carried out, extracting properties and characteristics for Larc SI, Larc TOR, M5 fiber, Dyneema, Aracon, Kapton and Kevlar, in particular. After analysing all advantages and disadvantages of the different designs, materials and tether configurations in the state-of-the- art, a tape tether has been selected as the most suitable configuration.

The tape will be manufactured in ALPET material. The ALPET is a commercial wire that is supplied by computer-systems companies. The ALPET comprises three different layers: the two external ones are manufactured in aluminium and have 10-12 μm of thickness, and the core is manufactured in PET and has 25-28 μm of thickness. The tape has a width of 25mm.

The tether will be divided in three main parts:

- A: it is joined to the Endmass and is non-conductive.
- B: it is situated between A and C and is conductive and bare.
- C: it is joined to the satellite and is an insulated conductive part.

All three A, B and C parts will be manufactured in ALPET. A dielectric material will be selected to coat the ALPET in C and will be also used to insulate A (it will be situated between A and B parts). In this way, the

ALPET can be installed in the non-conductive part of the tether.

The tape tether will be connected with the satellite by means of a belt fastening system. The other end of the tether will be joined to the deployer canister, which will also be used as Endmass. The canister will contain rough surfaces to brake the deployment of the tether and avoid transmitting all the impact forces of the deployment to the adhesive between tether and canister.

REFERENCES

[1] Ya.L. Al'pert, A.V. Gurevich, and L.P. Pitaevskii, Space Physics with Artificial Satellites, Consultants Bureau, New York, 1965.

[2] J.G. Laframboise, UTIAS Report No. 100, June 1966.

[3] M.J.M. Parrot, L.D. Storey, L.W. Parker and J.G. Laframboise, Phys. Fluids **25**, 2388 (1982).

[4] J.G. Laframboise and L.W. Parker, Phys. Fluids **16**, 629 (1973).

[5] J.-F. Roussel, F. Rogier, G. Dufour, J.-Ch. Matéo-Vélez, J. Forest, A. Hilgers, D. Rodgers, L. Girard and D. Payan, SPIS Open Source Code: methods, capabilities, achievements and prospects, IEEE Trans. Plasma Sc. **36**, 2360, 2008.

[6] J.-F. Roussel, G. Dufour, J.-Ch. Matéo-Vélez, B. Thiébault, B. Andersson, D. Rodgers, A. Hilgers and D. Payan, SPIS multi time scale and multi physics capabilities: development and application to GEO charging and flashover modeling, submitted to IEEE Trans. Plasma Sc.

[7] J.D. Williams and P.J. Wilbur, J. Spacecraft and Rockets **9,** 820 (1992).

[8] I. Katz, J.R. Lilley Jr., A. Greb, J.E. McCoy, J. Galofaro, D.C. Ferguson, J. Geoph. Res., **100**, 1687 (1995).

[9] C.L. Johnson, R.D. Estes, E. Lorenzini, M. Martinez-Sanchez, J. Sanmartin, J. Spacecraft and Rockets, **37**, 173 (2000).

[10] J.R. Beattie, W.S. Williamson, J. Matossian, E. Vourgourakis, J.L. Burch, and W.C. Gibson, "High-current plasma contactor neutralizer system," AIAA/ NASA/ASI/ESA, 3rd Intl. Conf. on Tethers in Space - Toward Flight, San Francisco, CA, May 17-19, p. 406, 1989.

[11] J.D. Williams and J.R. Beattie, "Spacecraft Potential Control using Plasma Contactors," 3rd International Workshop on the Interrelationship Between Plasma Experiments in the Laboratory and in Space, IPELS'94, Pitlochry, Scotland, July 24-28, 1994.

[12] D.E Parks, I. Katz, B. Buchholtz, and P.J. Wilbur, J. of Appl. Phys., **74-12**, 7094, 1993.

[13] P. Janhunen et.al., Rev. Sci. Instrum. **81**, 111301, 2010.

[14] GEMS – A mole to explore the interior of Mars, http://www.dlr.de/dlr/en/desktopdefault.aspx/tabid-10333/623_read-818/, 12.09.2011